Design, fabrication, and measurement of giant birefringence at telecommunications wavelengths in multi-slotted silicon nanophotonic optical waveguides

***Shayan Mookherjea*[1], *Michael L. Cooper*[1], *Jung S. Park.*[1], *Shun-Hui Yang*[2], *Prabhakar R. Bandaru*[2]**

[1] Micro-Nano Photonics Laboratory, University of California, San Diego,
Department of Electrical and Computer Engineering, Mail Code 0407, La Jolla, California 92093 USA.
Tel: (858) 534-4483, Fax (858) 534-1225, Email: mookherjea@ece.ucsd.edu

[2] University of California, San Diego, Department of Mechanical and Aerospace Engineering, Mail Code 0411, La Jolla, California 92093 USA. Tel: (858) 534–5325, Fax (858) 534–5698, Email: pbandaru@ucsd.edu

Abstract

Giant optical birefringence has been demonstrated in multilayer polymeric thin films (delta_n=0.3), in nanostructured silicon (delta_n=0.3) and in semiconductor nanowires (delta_n=0.8). In chip-scale waveguides at telecommunications-related wavelengths (1550 nm), giant birefringence has also been observed in the silicon-air slot waveguide (delta_n=0.7). Here, we demonstrate record giant birefringence (delta_n=1.5) over 60 nm of bandwidth near lambda=1550 nm in a multi-slotted silicon nanophotonic waveguide. For the first time, the measured birefringence spans a full octave (nTE = 2×nTM).

1. Introduction

The birefringence introduced in isotropic media by the periodic stacking of layers, called form-birefringence, can be utilized to propagate TE and TM wave with different effective phase velocities, such as used in dichroic polarizers, and in the synthesis of uniaxial crystals with prescribed properties. This capability is particularly useful for nonlinear optical wave generation in several commonly used semiconductors. Here, we demonstrate such capability in silicon, which is considerable interest for integrated optics nowadays. The form-birefringence is optimally engineered by deeply sub-wavelength channels of specific dimensions etched within a single-mode waveguide, which are strongly coupled in the near field.

Nanophotonic "void" or "slotted" waveguides [1,2], comprising alternate layers of low index (e.g., air or silicon oxide) and high index (e.g., Silicon) material, with cross-sectional features smaller than the wavelength of light, enable the concentration of electric field and enhanced power densities in the low index layers. Such features offer could be used for wavefront engineering, more efficient sensors, light trapping, nonlinear optics and radiation/coupling.

So far, single-slot waveguides have been proposed and experimentally demonstrated [1-3], and horizontally oriented multilayer structures been posited through numerical simulations [4]. Here, we propose and experimentally demonstrate vertically striped multi-slotted waveguides (see Fig. 1), where the superposition of the individual slot modes could be described in terms of supermode theory [5].

Further, we experimentally measured the group index of fabricated multi-slotted waveguides in silicon in close agreement over a wide range of wavelengths with the simulation results carried out using a commercial finite-difference mode-solver software package. Finally, we also design and demonstrate mode shaping of both the TE and TM polarizations to achieve near-identical coupling to a macroscopic external object, such as a lensed fiber or detector.

2. Theory: Eigen-modes of multi-slot waveguides

The transverse cross-section of the multi-slot structure (see Fig. 1c) consists of high-index cores separated by low-index claddings. The waveguiding formalism of the composite structure is described by supermodes [5,6], and yields, as the main result of interest, that *in the high index regions,* the peak field amplitudes for the m-th order mode (for $E_y^{(m)}$ in the TE polarization or $H_y^{(m)}$ in the TM polarization) should obey the inter-relationship $c_n^{(m)} = \sin[\pi n(m+1)/(N+1)]$ where n = 1, 2, …, N (number of identical waveguides) and indicates the coefficients of the individual eigenfunctions constituting the supermode.

For modeling purposes, in the transverse cross-section, our structures consist of five identical (N=5) high-index (n_{core}=3.48) sections separated by low-index (n_{clad} =1.45) gaps. For the fundamental (m=0) modes, the prediction of supermode theory is that $c_n=\left\{1/2, \sqrt{3}/2, 1, \sqrt{3}/2, 1/2\right\}$. Using a mode-solver program to calculate the modes, we show in Fig 1e that the peaks closely satisfy the expected ratios (a small correction could arise from next-to-nearest neighbor coupling); thus the supermode framework is applicable in this waveguide geometry, and can be used in the future to analyze and design multi-slotted structures. Note, as observed before [1-4], that the field component $|E_x|$ for the TM polarization is greatly enhanced (by a factor n_{core}^2/n_{clad}^2 at the edges) in the low-index cladding regions, as required by continuity of the normal electric displacement across the boundary.

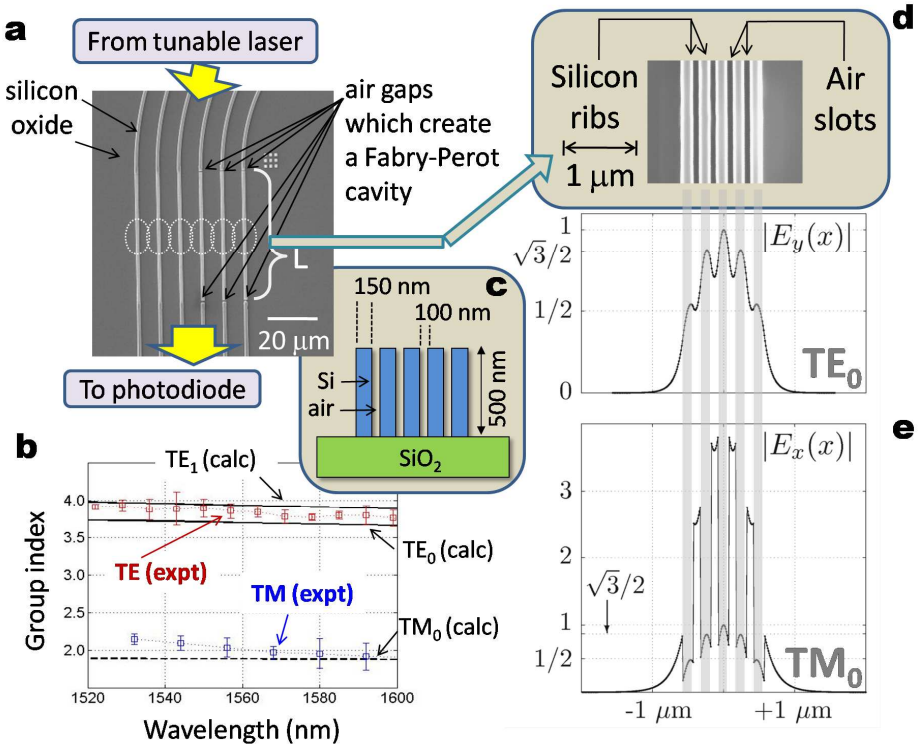

Fig. 1 a: Scanning electron microscope (SEM) image of a silicon-on-insulator (SOI) chip containing six multi-slot waveguides. (The waveguides complete a 90° bend to the top-right before terminating at the cleaved facet.) Three of the waveguides on the right have 0.4 μm air gaps separating from them from the conventional silicon waveguides, thus creating a Fabry-Perot resonator of length L. **b**: Magnified SEM image of the multi-slot waveguide. **c**: Schematic of the transverse cross-section. **d**: Measurement (labeled 'expt') of the group index $n_g(\lambda)$ for the TE and TM polarizations. Both the TE_0 and TE_1 modes could be excited in the slotted structure by the input waveguide. The simulations (labeled 'calc') are performed using a finite-difference photonic simulation software package. **e**: field amplitude profiles for the transverse electric field component of the (fundamental) TE_0 and TM_0 eigenmodes. The ratio of field amplitudes in the individual high-index regions, calculated by a vectorial finite-difference mode-solver, follows the supermode progression, sin (nπ/6) (n = 1 to 5).

3. Experiment: fabrication and measurement

Using electron-beam lithography and dry etching, multi-slot waveguides consisting of four air slots in a silicon core were fabricated on a silicon-on-insulator (SOI) wafer, with silicon thickness of 500 nm, slot width 100 nm and slot-to-slot spacing of 150 nm (see Fig. 1c). Coherent light from a narrow-band tunable laser was coupled into a waveguide through polarization maintaining fiber and silicon waveguide tapers, and the transmission was measured using an InGaAs photodiode.

In order to measure the group indices of the slotted waveguide sections, the multi-slot section was separated from the normal input/output waveguides by short (0.4 μm) air gaps, so that a Fabry-Perot resonator is created along the waveguiding direction. (Waveguides with and without these gaps are shown in Fig. 1a). The measured transmission spectrum was bandpass filtered in the spectral domain to extract that frequency component which corresponds to the Fabry-Perot resonances of the length *L* indicated in Fig. 1a.

From these resonances, we obtained the group index of the structure in both the TE and TM polarizations over a bandwidth of about 80 nm (see Fig. 1b), and the experimental values agree closely with computational simulations, which were obtained by taking into account the fact that the bottom cladding (silicon dioxide) has a different refractive index than the top and side claddings (air). (Note that if such a waveguide is used to make, for example, a microring add-drop filter, it is the group index, and not the effective index as in a thin-film structure, that determines the free-spectral range, the finesse, and other spectral figures-of-merit.) We measure an engineered birefringence (refractive index difference between TE and TM) delta_$n_{TE\text{-}TM}$~1.5 over more than 60 nm bandwidth.

As shown in Fig. 1e, the TE and TM modes have very different profiles in the near field. Direct butt-coupling to another optical element with small numerical aperture (typical for on-chip components as well as off-chip detectors and couplers) would create a large polarization-dependent loss. However, since in both polarizations, the peak field amplitudes in the high-index regions follow the supermode progression described earlier it is possible to create an imaging system to shape the modes so as to achieve near-identical coupling to an external detector, fiber coupler, or optical element. The main function of the beam-shaping optic is to cut-off high spatial frequencies, and it may be designed either on-chip or off-chip. Provided that the cut-off frequency is chosen high enough, the measurement can also be used to verify that the higher-order TE1 mode is not excited in the waveguide and eliminate a potential concern since, as shown in Fig 1b, the theoretically-predicted indices are similar for the TE0 and TE1 modes.

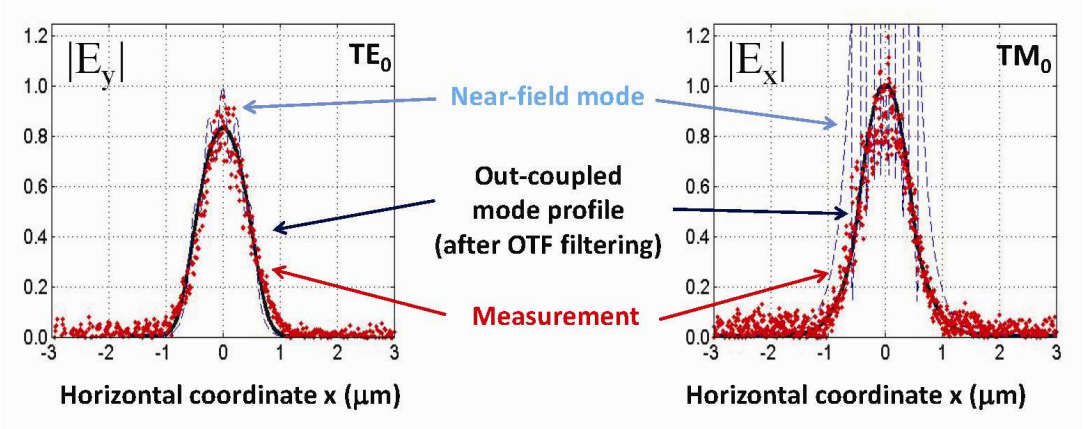

Fig. 2 Mode profiles from a vectorial finite-difference calculation (dashed blue line). The black line shows the fields as should be observed by a diffraction-limited imaging system with focal length f=2 mm, numerical aperture NA=0.55, and exit aperature 0.5 mm at a distance of 2.5 cm from the exit aperature. The red squares are experimental measurements using a Mitutoyo SL100x ULWD objective followed by a Navitar UltraPreciseEye 2x magnification tube lens (total magnification 181x), and imaged onto a New Focus Femtowatt photoreceiver. The mode profile is obtained by the scanning knife-edge method. Field profiles are obtained from the scanning traces by differentiation and filtering out the high-frequency components which have spatial frequency > 200 /cm, attributing these high-frequency components (more than 3 times the cut-off frequency of the OTF) to random deviations from linearity in the mechanical movement of the translation stage.

The center-to-center distance between the two intensity peaks of the TE1 mode is about 0.65 um, which is less than Abbé resolution limit for two point sources at a wavelength of 1.55 um. However, the two lobes of this mode are in phase opposition (exactly pi out of phase with regard to each other), and under these conditions, the diffraction-limited image (post OTF-filtering at the image plane, which has a principal frequency component at 85 /cm) should show a dip at the center [7]. Such a pattern was not observed in the measurements as shown in Fig. 2. We conclude that, as expected from the symmetry the field in the launching waveguide, the TE1 mode was not excited in the multi-slotted waveguide.

5. Conclusion

In conclusion, we measure a giant engineered form-birefringence, delta_n=1.5 (refractive index difference between TE and TM) over more than 60 nm bandwidth at wavelengths of importance in telecommunications (1530-1590 nm). When combined with refractive index modulation (thermal or electro-optic), such a large artificially-induced birefringence could be utilized for very compact chip-scale optical delay lines and waveguide-based polarization switches incorporating phase retardation, and for phase-matching between waves over a very wide range, determined by the widths and spacing of the multiple high-index ribs and low-index slots which comprise the waveguide. The design principles can be easily scaled and adapted to create giant birefringence in any material system which can be lithographically patterned and etched at sub-micron dimensions.

6. Acknowledgments

This work was supported by the National Science Foundation (NSF) under grants ECCS-0642603 and ECCS-0403589. JSP acknowledges support provided by the NSF Graduate Student Research Fellowship.

7. References

1. V. R. Almeida, Q. Xu, C. A. Barrios and M. Lipson, "Guiding and confining light in void nanostructure" *Opt. Lett.* Vol. 29, pp. 1209-1211 (2004)

2. Q. Xu, V. R. Almeida, R.R. Panepucci and M. Lipson "Experimental demonstration of guiding and confining light in nanometer-size low-refractive-index material" *Opt. Lett.* Vol. 29, pp. 1626-1628 (2004)

3. T. Baehr-Jones, M. Hochberg, C. Walker, A Scherer, "High-Q optical resonators in silicon-on-insulator-based slot waveguides" *Appl. Phys. Lett.* Vol. 86(8), art. 081101 (2005)

4. N. N. Feng, J. Michel, and L.C. Kimerling, "Optical field concentration in low-index waveguides" *IEEE J. Quantum Electron.*, Vol. 42, pp. 885-890 (2006)

5. A. Yariv, Optical Electronics in Modern Communications, 5th edition, (Oxford, New York, 1997), Section 13.9

6. G. Lenz and J. Salzman, "Eigenmodes of multiwaveguide structures" J. Lightwave Tech., Vol. 8(12), pp. 1803-1809 (1990)

7. J. W. Goodman, *Introduction to Fourier Optics* (McGraw-Hill, New York, 1988), Fig. 6-11.